Solvation Dynamics in Protein Environments Studied by Photon Echo Spectroscopy

Xanthipe J. Jordanides,[†] Matthew J. Lang,[‡] Xueyu Song,[§] and Graham R. Fleming*[,†]

Department of Chemistry, University of California, Berkeley and Physical Biosciences Division, Lawrence Berkeley National Laboratory, Berkeley, California 94720, Department of Molecular Biology and Princeton Materials Institute, Princeton University, Princeton, New Jersey 08544, and Department of Chemistry, Iowa State University, Ames, Iowa 50011

Received: March 30, 1999; In Final Form: July 14, 1999

Photon echo spectroscopy is used to study the mechanisms of solvation dynamics in protein environments at room temperature. Ultrafast and additional multi-exponential long time scales are observed in the three-pulse photon echo peak shift data of the fluorescein dye eosin bound to lysozyme in aqueous solution. The dynamics of the solvated lysozyme are characterized with dielectric continuum models that integrate dielectric data for water with that for lysozyme. By comparing our data with previous results for eosin in water [Lang, M. J.; Jordanides, X. J.; Song, X.; Fleming, G. R. *J. Chem. Phys.* **1999**, *110*, 5584], we find that the total coupling of the electronic transition frequency of eosin to the nuclear motions of the aqueous lysozyme solution is smaller than in the aqueous solution. On an ultrafast time scale, solvation appears to be dominated by the surrounding water and not by the ultrafast internal motions of lysozyme. However, over long time scales, lysozyme does contribute significantly, either directly through motions of polar side chains or indirectly through reorientation of the water "bound" to the surface of the protein.

I. Introduction

Central to the understanding of chemical dynamics in condensed phases is the understanding of how solvent dynamics influence the energy fluctuations of solvated macromolecules. Such energy fluctuations allow reactants to surmount potential energy barriers and remove excess energy to stabilize products.

The fluctuations of electronic energy gaps of medium-sized solutes in polar solvents have been extensively characterized experimentally,[1−3] theoretically,[4−7] and computationally.[8] If adequate dielectric data for the solvent are available, the electronic energy fluctuations of the solute can be predicted with reasonable confidence. Similar fluctuations of solvated biological molecules have also been described. For example, the energy level fluctuations of prosthetic groups involved in electron or energy transfer have been simulated,[9,10] substrate energy fluctuations have been invoked in catalytic processes such as hydrogen transfer processes,[11] and the fluctuations in the barriers for rebinding of small molecules such as CO to myoglobin have been studied by nonlinear spectroscopy.[12,13] However, unlike the comparatively simple system of a medium-size solute in a polar solvent, the time scales and magnitudes of the energy fluctuations of a chromophore within a biological macromolecule have yet to be completely characterized. As a first step toward characterizing the dynamics of a biological macromolecule in water, the present work investigates the time scales and magnitudes of the energy fluctuations of a chromophore bound to a solvated protein.

Several questions immediately arise: (1) Are the time scales and magnitudes of the energy fluctuations of a chromophore (or more specifically the spectroscopically observable electronic energy gaps) dominated by the local or long-range interactions with the protein? (2) Are these energy fluctuations affected by surrounding water? (3) If water does contribute substantially, are these fluctuations due to long-range interactions with the bulk water, (whose dielectric response is dominated by an ultrafast (∼30 fs) component, and whose relaxation is complete by ∼15 ps)[14,15] or are they due to short-range interactions with the water of hydration—water associated with charged residues on the surface and within the protein (bound water)?[16]

Recently, evidence that local protein motions influence the electronic energy levels of bound chromophores has emerged. In photosynthetic systems for example, where chromophores are bound to nonpolar regions of the protein, an ultrafast (<100 fs) inertial protein response has been suggested from both simulation[9,10] and experimental investigations.[17−19] Homoelle et al. have suggested that dynamical fluctuations observed in phycobiliproteins involve either motions of local amino acids or motions of water molecules that line the chromophore binding site.[20] In addition, Fraga and Loppnow have shown that internal protein motions as far as 12 Å from the chromophore can couple to the transition frequency, thereby contributing to the protein reorganization energy.[21] In order to estimate the coupling between the charge distributions of chromophores and those of the protein, a complete knowledge of the protein dielectric response is required.

A substantial theoretical effort has been directed toward the characterization of the dielectric and electrostatic properties of proteins.[22−25] For example, Warshel and co-workers used microscopic molecular dynamics (MD) simulations of trypsin to show that the protein dielectric constant varies with site: it can be as large as 11 for a catalytic site and as small as 4 for a nonfunctional site.[23] Also using MD simulations, Van Gunsteren and co-workers calculated a dielectric constant of 30 for lysozyme in water, which was ascribed to side chain fluctuations.[24] A more detailed model might be to order the protein in discrete regions of progressively increasing dielectric constants with the largest response arising from the combined contribu-

* Corresponding author e-mail address: GRFleming@lbl.gov.

10.1021/jp9910993 CCC: $18.00
Published on Web 09/01/1999

tions of polar surface side chains and their associated water molecules.[25] MD simulations of six proteins in water by Brooks and co-workers show that the dielectric constant is largely dominated by the charged residues at the protein surface and ranges from 11 (myoglobin) to 21 (cytochrome *c*).[25]

The experimental literature does not allow simple conclusions to be drawn with regard to the dielectric and electrostatic interactions in proteins.[26−34] Dielectric measurements of aqueous lysozyme (95 wt % water)[26−29] and of hydrated lysozyme powder (34−54 wt % water)[30−32] yielded substantially different results − perhaps because of differing degrees of hydration of lysozyme or a varying electric field strength.[35] Likewise, there is no consensus on the physical assignments of specific dielectric dispersions. For example, the origin of the increase in polarizability with increasing hydration is ascribed either to dipolar water molecules[30] or to changes in the vibrational freedom of amino acids.[31,32]

Extensive experimental work shows that the structure and dynamics of water in the hydration shell differ from the structure and dynamics of bulk water. For example, X-ray and neutron scattering data for an aqueous lysozyme solution show that a hydration shell of approximately 3 Å thickness is significantly more dense than bulk water.[36] Various NMR studies of sequentially hydrated lysozyme also support the presence of a hydration layer but yield several different relaxation times.[33,34] One NMR experiment reported time constants of 10 ps, 2 ns, and 1 μs.[33] Later, a similar NMR measurement resolved 17, 27, and 41 ps relaxation times.[34] Both experiments on hydrated lysozyme assign the physical origin of the time scales to different classes of water associated with lysozyme. Dielectric spectroscopy experiments probing molecular orientational relaxation also yield multiple relaxation time scales. In the first dielectric measurement of a protein (myoglobin) in an aqueous solution, Grant attributed the four observed dielectric relaxation time scales to: (1) reorientation of bulk water (8 ps); (2) reorientation of the entire protein molecule (15 ns); and (3) relaxation of the water associated with the protein (10 ps, 150 ps).[37] Although the 10 and 150 ps components corroborated the existence of bound water, other explanations for the bimodal nature of the intermediate relaxation times are also plausible. For example, they may be associated with the dynamic equilibrium between the free and bound water molecules.[16] In accordance with the above results from experiments (dielectric, NMR) and MD simulations, protein relaxation is quite complex, involving many correlated motions of many atoms along many coordinates.

The present photon echo measurements aim at characterizing the magnitudes and time scales of energy fluctuations of the chromophore eosin bound to lysozyme in aqueous solution at physiological temperature. Eosin bound to lysozyme is henceforth called the lysozyme complex and is shown in Figure 1. This system was selected because of extensive spectroscopic characterization[38−41] and because a detailed experimental and theoretical study of the solvation dynamics of eosin in a dilute aqueous solution has been completed.[14] No single experimental approach is likely to cover all of the characteristic time scales of the interatomic forces in a solvated protein since the range of time scales is so broad, from tens of femtoseconds to microseconds. However, three-pulse photon echo peak shift (3PEPS) allows for observation of the electronic energy gap fluctuations from 10 fs to hundreds of nanoseconds.[42,43] These 3PEPS results are discussed in terms of dielectric continuum models including contributions from protein/chromophore, protein/water, and chromophore/water interactions.

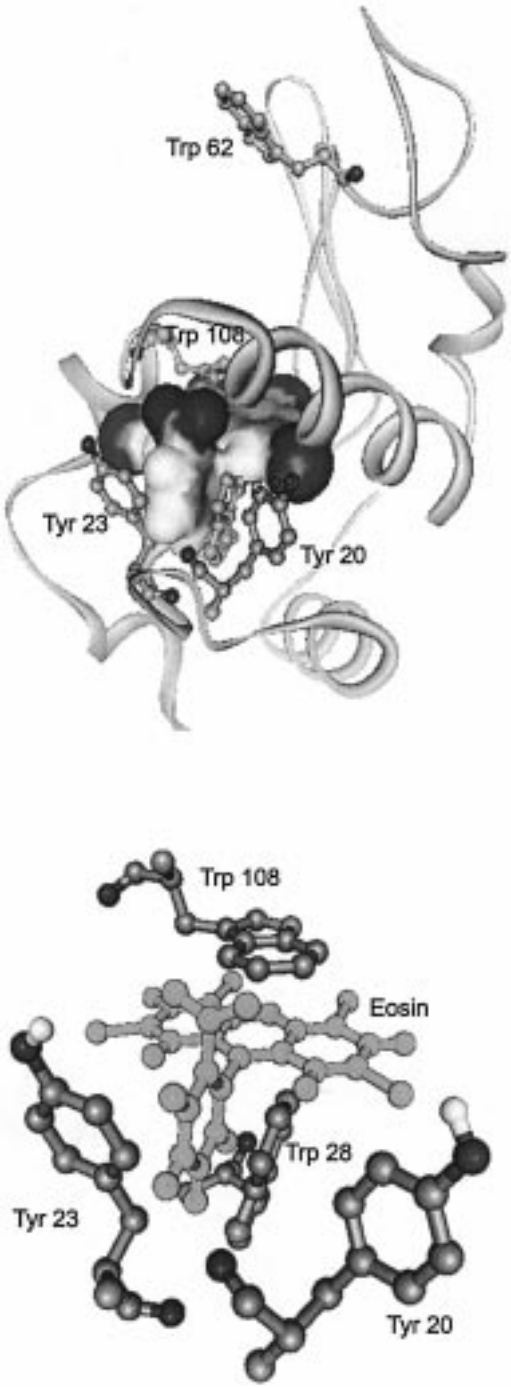

Figure 1. The structure of the lysozyme complex as described by Baugher et al.,[39] with the lysozyme X-ray crystal structure after Ramanadham et al.[46] The eosin chromophore, depicted using a van der Waals surface, is bound to the "hydrophobic pocket" of lysozyme defined by residues Trp 28, Trp 111, Tyr 22, and Met 105. The eosin is coplanar with Trp 108 and 13 Å from the Trp 62 (upper panel). Detailed view of the binding site: Tyr 20 and Tyr 23 can form two hydrogen bonds with the two oxygen atoms of eosin. The hydrogen atoms of the two Tyr residues are shown for clarity (lower panel).

II. Methods

A. Experimental. *1. Lysozyme*. Spectroscopic measurements were performed with 3X crystallized, dialyzed, and lyophilized chicken egg white lysozyme (used as received from Sigma), eosin Y (Sigma) purified by recrystallization from acidic solution, and triply distilled water. The sample was filtered through a 0.22 μm membrane filter and centrifuged before loading in a 100 μm path length flow cell. Concentrations

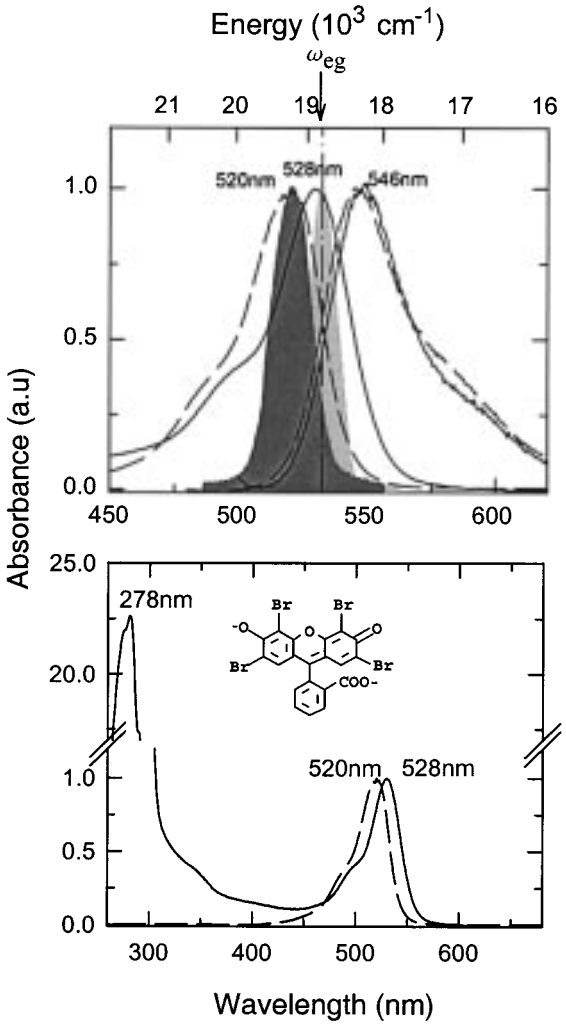

Figure 2. Absorption spectra of eosin (structure shown) in water centered at 520 nm (dashed line) and the red-shifted lysozyme complex centered at 528 nm (solid line), together with the corresponding fluorescence spectra. The frequency where the absorption spectrum and the fluorescence spectrum intersect, ω_{eg}, is ~19 000 cm^{-1} (used in the Appendix). The dark gray and light gray shaded portions are the laser spectra (upper panel). The 278 nm peak of the lysozyme complex arises from the ultraviolet absorbing protein residues Tyr and Trp (lower panel).

of the aqueous solutions were spectroscopically determined by the ratio of the eosin absorption peak at 530 nm to the tryptophan (Trp) and tyrosine (Tyr) absorption in lysozyme at 280 nm as shown in the lower panel of Figure 2. Peak shift measurements were obtained with 15−20 mL sample solutions having an optical density of 0.08 at the absorption maximum.

Previous spectroscopic studies have shown that eosin, a fluorescein derivative, forms a 1:1 complex with lysozyme, without inhibition of enzymatic activity.[38,39] In addition, eosin has been shown to have one spectroscopically unique lysozyme binding site.[38,40,41] Results obtained by Grossweiner and co-workers, first via photodynamic inactivation studies[38] and later with a study of energy transfer from tryptophan to eosin,[39] strongly suggest that eosin binds in a "hydrophobic box" of lysozyme. This hydrophobic box was first pointed out via X-ray crystallography[44] and has properties corroborating the spectroscopic results of Grossweiner and co-workers.[38,39] The hydrophobic box is defined by the midpoint of a box composed of Trp 28, Trp 111, Tyr 23, and Met 105 and lies coplanar with Trp 108 as shown in Figure 1.[38,39,44] This pocket is located close to the enzyme surface with Trp 108 on the inside wall, behind the active site, and it accommodates a planar eosin that lies at the midpoint of the box.[38,39] As shown in the lower panel of Figure 1, Tyr 20 and Tyr 23 are in favorable positions to hydrogen bond with the two partially charged xanthene oxygens of eosin as previously suggested.[41]

To ensure that all the eosin was bound to lysozyme, the eosin concentration was fixed to 8.3×10^{-5} M (96% bound). To prevent the presence of protein dimers, the concentration of lysozyme was fixed to 2.6×10^{-3} M, well below the concentration at which it dimerizes.[40] Next, measurements were made in unbuffered solutions at pH 5.3 since the maximum binding ($K_b = 3\ \mu$M) was shown to occur at pH 5.3 where the net charge on the protein is positive (I. P. 11) and the charge on eosin is minus two.[38]

2. 3PEPS Measurement. The three-pulse photon echo peak shift (3PEPS) measurements employed here have been described extensively elsewhere.[42,43] In short, the laser pulse is split into three equal energy pulses aligned in an equilateral triangle geometry. Two pulses travel over variable delay lines providing the two experimentally controllable time periods: the coherence period τ, the time delay between the first and second pulses, and the population period T, the time delay between the second and third pulses. The first pulse creates a coherence or superposition between ground and excited states, the second creates a population, either in the ground or excited state, and the third again creates a coherence. If the phase during the second coherence period is the complex conjugate of the first, the sample generates a coherent echo field at some time t after the last pulse. In a 3PEPS experiment, the integrated photon echo signal, collected in two phase-matched directions, is measured as a function of fixed delay T while scanning τ. The peak shift is defined as half the time difference between the two phase-matched echo signals as a function of population time T.

The Coherent laser system used in these experiments has been described previously.[45] In short, a mode-locked Ti:sapphire oscillator (Coherent Mira) was used to seed the regenerative amplifier (Coherent RegA-9050). The 800 nm RegA pulses were then used to pump a double pass optical parametric amplifier (Coherent OPA-9400). The laser system generates 40−50 fs Gaussian transform-limited pulses with an energy of ~50 nJ (stability, ± 3%) at a repetition rate of 250 kHz. The frequency spectra of the pulses are shown by shaded regions in the upper panel of Figure 2. In these measurements, the optical parametric output was tuned to 530 nm for the aqueous lysozyme complex and 520 nm for eosin in water. The autocorrelations of the pulses at both 520 and 530 nm were identical.

B. Theory. Song and Chandler have developed a dynamic dielectric continuum model to calculate the time-dependent solvation energies for an arbitrary charge distribution in a dielectric cavity of a realistic molecular shape.[7] If lysozyme can be viewed as a dielectric continuum with a specific dielectric response, this theory can be applied to calculate the solvation energies of the solute eosin embedded in a hydrophobic pocket of the solvated lysozyme protein.

Modeling of the lysozyme complex in water to obtain a theoretically calculated peak shift proceeded as follows. For the lysozyme complex in water, the coordinates and charge distribution of eosin in both the ground and excited states were estimated using MOPAC.[14] Atomic coordinates of lysozyme were obtained directly from the X-ray crystallographic structure.[46] Frequency-dependent dielectric data for water[47] and

lysozyme were obtained from experiment[30] and MD simulation[24] as discussed in section III B. Each atom of eosin and lysozyme was modeled as a sphere with a given van der Waals radius. A Lee and Richards molecular surface was generated to obtain the boundary of the dielectric protein cavity.[48] The time dependent solvation energy of the chromophore−protein complex can be calculated using the charge distribution of eosin, the molecular surface of the lysozyme complex, and the dielectric data for both lysozyme and water according to the method in refs 7 and 14.

Once the solvation energy of the system is calculated, the imaginary part of the solvation energy $E''(\omega)$ is readily related to the spectral density $\rho(\omega)$ according to

$$\rho_{sol}(\omega) = E''(\omega)/\omega^2 \tag{1}$$

as derived in section V of ref 14. The spectral density characterizes the range and distribution of frequencies of the response weighted by how strongly each frequency couples to the electronic transition frequency. This weighting of the spectral density is also referred to as the coupling strength $\langle\Delta_i^2\rangle^{1/2}$, which in the high temperature limit has a simple relationship to the reorganization energy λ according to[49,50]

$$\langle\Delta_i^2\rangle = 2\lambda k_b T/\hbar \tag{2}$$

It is important to note that the spectral density presented here is not based on an assumption of harmonicity of the molecular motions. The spectral density for a harmonic system is temperature independent. However, the spectral density used in our formalism derives from experimental dielectric data and not from a harmonic model (e.g., instantaneous normal modes or multimode Brownian oscillators). Because the experimental dielectric data are temperature dependent, the calculated spectral density will be temperature dependent. After applying the quantum fluctuation−dissipation theorem, the line broadening function, calculated according to eq A6, is readily obtained from $\rho(\omega)$. Using a second-order cumulant expansion, the response functions of linear and nonlinear spectroscopies, in particular the three-pulse photon echo signal, can then be calculated for comparison with experiment.[49,50]

III. Results

A. Experimental. *1. Steady-State Spectra*. Absorption and fluorescence spectra of the solvated lysozyme complex and of eosin in water, as well as the spectrum of the laser pulses, are shown in the upper panel of Figure 2. The lysozyme complex absorption spectrum is red-shifted by 350 cm^{-1} with respect to the eosin/water spectrum. A similar red-shift is seen in many other protein/chromophore systems and will be addressed in section IV A. These absorption and fluorescence spectra are also used to calculate the reorganization energies. From the normalized first moment of the difference between the absorption and fluorescence spectra, the reorganization energy can readily be calculated according to eq A12 as derived in the Appendix. The reorganization energies for eosin in water and for the lysozyme complex in water are 877 cm^{-1} and 710 cm^{-1}, respectively. The coupling strengths can be readily calculated via eq 2 and are 3.6×10^5 cm^{-1} for eosin in water and 2.9×10^5 cm^{-1} for the lysozyme complex in water. Hence, the experimental steady-state absorption and fluorescence spectra indicate that coupling strength is lower in the eosin in water system than in the lysozyme complex.

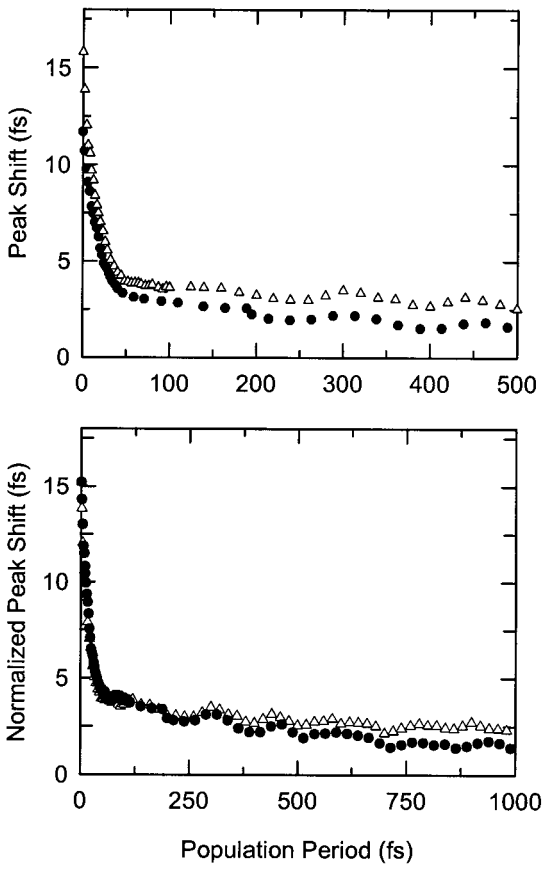

Figure 3. Comparison of the eosin in water three-pulse photon echo peak shift (solid circles) with that of the lysozyme complex (open triangles, upper panel). The two data sets are normalized to the same initial value and reveal similar behavior of both the ultrafast dynamics and the intramolecular vibrational coherences (lower panel).

2. Peak Shift Measurements. Three-pulse photon echo peak shift data for both eosin and the lysozyme complex in water are shown in the upper panel of Figure 3. The initial peak shifts for eosin in water and for the aqueous protein complex are ~12 fs and ~16 fs, respectively. The initial peak shift has been shown to be sensitive to the mean square fluctuation amplitude of the transition frequency, i.e., the coupling strength. Dependence of the initial peak shift on the pulse duration and the bath correlation time is also recognized.[42,43] Hence, the increased initial peak shift in the protein complex can be attributed to a decreased total coupling strength. This interpretation is supported by smaller reorganization energies obtained for the complex from steady-state absorption and fluorescence spectra. The ultrafast decay in the peak shift, within < 10 fs, is due to destructive interference between the high-frequency intramolecular vibrational wave packets,[42,43] or possibly intramolecular vibrational energy distribution,[51] and is commonly observed.[19,20,42,43,50−52] The lower panel of Figure 3 shows the peak shift of eosin in water when normalized to the initial peak shift value of the lysozyme complex in water. It enables a clear comparison of both of the oscillations reflecting the vibrational coherences and the ultrafast decay. These vibrational coherences appear to be nearly identical; hence, the presence of the protein environment does not appear to significantly alter either the frequencies or damping times of the intramolecular vibrations of eosin.

The data show that the initial solvation occurs on an ultrafast time scale for eosin in water and eosin bound to lysozyme in water. In a recent study, we showed that a substantial amplitude (~60%) of aqueous solvation occurs within ~30 fs.[14] This

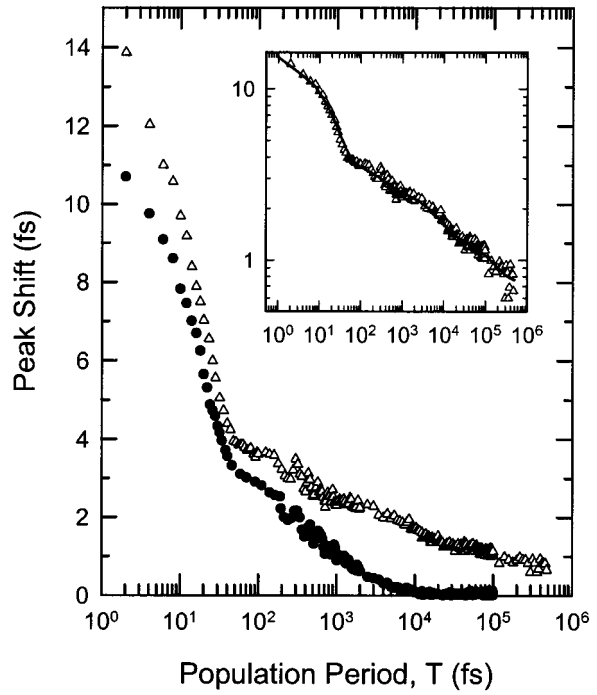

Figure 4. Logarithmic (log) plot of the peak shift data of eosin in water (solid circles) and lysozyme complex in water (open triangles). The inset is a log−log plot of the lysozyme data (open triangles) is shown with fit (solid line).

ultrafast response has been attributed to the two high-frequency intermolecular solvent bands of water: the hindered translation stretch of the H-bonding network at 180 cm^{-1} and the librational band at 600 cm^{-1} (both shown in the water spectral density in the lower panel of Figure 6).[4] For a more precise comparison of the ultrafast component in both systems, the initial peak shifts were normalized, and the short time dynamics are shown in the lower panel of Figure 3. After normalization, the initial dynamics appear quite similar up to 200 fs and begin to diverge thereafter. Between 200 and 1000 fs the peak shift of eosin in water has decayed from 3 to 1 fs, whereas that of the lysozyme complex in water has only decayed from 3 to 2.5 fs.

The logarithmic plot in Figure 4 clearly shows the marked difference in the long time dynamics of the two systems. The solvated eosin/lysozyme peak shift reveals complex long time dynamics, whereas the peak shift of eosin in water completely decays by ∼15 ps. Moreover, a nonzero peak shift persists over the entire dynamic range of the eosin/lysozyme measurement (∼1 ns in the longest scans, not shown). This nonzero value of the peak shift at long population times in the lysozyme complex indicates either relaxations on time scales much longer than 1 ns or perhaps "static" (i.e., on time scales of minutes or hours) inhomogeneity. In this aqueous lysozyme solution the former explanation is more favorable.[17−20,53−57]

For a preliminary comparison of the time scales, global exponential fits to the experimental data were performed. A three-exponential fit (up to 100 ps) of the eosin in water data yields 17 fs (0.73), 330 fs (0.15), and 3 ps (0.12) with the relative amplitudes given in parentheses. A fit of similar quality for the aqueous lysozyme complex up to 500 ps, shown with the data in the inset of Figure 4, required four exponentials and yields 18 fs (0.69), 310 fs (0.09), 7 ps (0.08), and 135 ps (0.08). Hence, the majority of the relaxation amplitude in the aqueous protein system occurs on an ultrafast time scale. The two shortest time constants are clearly similar in the eosin/lysozyme data and the eosin in water data; however, longer time scales are evident in the peak shift of the aqueous lysozyme complex. Such multi-exponential behavior of the long time dynamics in proteins has previously been observed.[13,53] The longest time constant was reproducible in fits of the peak shift data up to 500 ps. However, a fit of an echo measurement up to 1 ns provides an even longer time component of ∼535 ps (contributing to ∼8% of the amplitude) instead of the ∼135 ps component. Because of the multi-exponential nature of the long time behavior, the time constants vary with the time scale of the fitting range. Although an exponential fit to the peak shift data does not provide accurate short time scales, the peak shift is directly related to the solvation correlation function, $s(t)$, for time scales longer than the bath correlation time.[1] The physical origins of the long time behavior in the lysozyme complex will be further investigated in section IV C.

B. Model Calculations. The frequency-dependent dielectric function, $\epsilon(\omega)$, of a protein is a measure of the polarizability of the protein media and is the appropriate macroscopic quantity to measure protein fluctuations. Although it is a challenge to obtain a reliable $\epsilon(\omega)$ for a protein, an extensive experimental pursuit to measure the dielectric function of lysozyme continues.[26−34] Among the most comprehensive are the dielectric dispersion measurements of Harvey and Hoekstra on hydrated lysozyme powders.[30] These dielectric dispersion measurements cover the frequency range from 10^7 to 2.5×10^{10} Hz. In addition, the molecular dynamics simulation results of van Gunsteren and co-workers of aqueous lysozyme calculate $\epsilon(\omega)$ from 10^5 to 10^{12} Hz. [24] This calculation uses a 1 ns simulation for lysozyme in an explicit solvent environment of 5345 water molecules and is one of the most comprehensive MD simulations of lysozyme. Hence, these are the two sources of information on the dielectric properties of lysozyme used to model the peak shift data.

Before applying the $\epsilon(\omega)$ results detailed above to the dynamic dielectric continuum theory of Song and Chandler, the solvation times of the frequency-dependent dielectric responses will be compared with those obtained in the three-pulse photon echo peak shift measurements. The dielectric measurements of Harvey and Hoekstra have two dispersions with longitudinal relaxation time constants of ∼16 ps (with a high-frequency dielectric constant ϵ_∞ of 2 and a low-frequency dielectric constant ϵ_s of 9) and ∼650 ps (with $\epsilon_\infty = 6$ and $\epsilon_s = 15$). When these time constants are converted from Debye relaxation times τ_D to solvation relaxation times, using the Debye formula for a dipole in a spherical cavity $\tau_{solvation} = \tau_D\ (\epsilon_\infty^i + 1)/(2\epsilon_s^i + 1)$, they yield values of ∼4 ps and ∼270 ps, respectively. In their measurement, the static dielectric constant is 15 corresponding to ϵ_s of the lowest frequency dispersion. The approximate solvation components of 4 and 270 ps compare reasonably well with the 7 and 135 ps solvation components obtained from the multiexponential fit to the lysozyme complex peak shift data. The molecular dynamics simulation obtained a much larger static dielectric constant of 30.[24] The frequency-dependent dielectric function of this simulation provides a single dielectric dispersion time constant of 1753 ps (with $\epsilon_\infty = 1.5$ and $\epsilon_s = 30$) corresponding to a solvation relaxation time of ∼100 ps that can be compared to the longer ∼270 ps relaxation in the peak shift measurements.

In an attempt to explore the complexity of the electrostatic and dielectric properties of proteins, we now construct four dielectric continuum models using the spectral density to calculate the three-pulse photon echo signal of the lysozyme complex. They are schematically shown in Figure 5. Each model

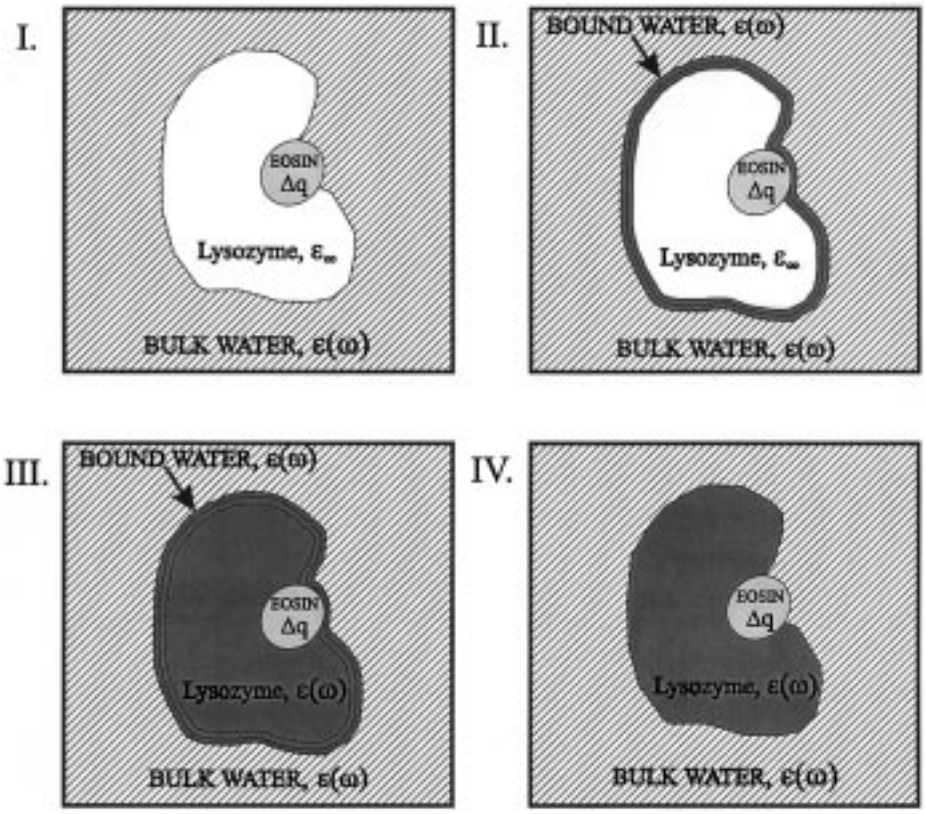

Figure 5. Schematic representations of the dielectric models used to simulate the peak shift data. In all models the same perturbation is used (see text). Model I treats lysozyme as a static dielectric cavity in an aqueous dielectric medium $\epsilon(\omega)$. Model II also includes the dielectric response of two layers of water associated with the protein, $\epsilon(\omega)$. Model III includes all of the above in addition to treating the entire lysozyme cavity with a frequency-dependent dielectric response, while model IV excludes the associated water. Models II and III use the lysozyme $\epsilon(\omega)$ obtained from experimental dielectric data of lysozyme,[30] whereas model IV uses the lysozyme $\epsilon(\omega)$ obtained from molecular dynamics simulations of lysozyme in water.[24]

uses the same perturbation, the same charge distribution for eosin, the same spectral density for the intramolecular vibrations of eosin, and the same dielectric continuum treatment of the bulk solvent. The total reorganization energy used in each model spectral density was constrained by that determined from experiment: $\lambda = 710$ cm^{-1} (see Appendix). The intramolecular vibrational and intermolecular solvation contributions to the spectral density are shown in Figure 6 with $\lambda = 110$ and 600 cm^{-1}, respectively. The upper panel of Figure 6 includes the intramolecular and intermolecular spectral densities on a logarithmic scale, while the lower panel shows only the intermolecular spectral densities. The peak shift simulations in Figure 7 include the water intermolecular solvation spectral density, while those presented in Figure 8 also include the intramolecular vibrational spectral density of eosin.

The first model treats lysozyme as a static dielectric cavity $\epsilon_\infty = 2$ in an aqueous dielectric medium. The spectral density (with $\lambda = 600$ cm^{-1}) and the peak shift of model I are identical to those for eosin in water and are shown by the gray lines in Figures 6, 7, and 8. As expected, model I fails to reproduce the long time behavior of the aqueous lysozyme complex. The second model again treats the protein cavity as a static dielectric medium ($\epsilon_\infty = 2$), but includes the dielectric response of two layers (4.5 Å) of water associated with the protein. The dielectric response of the first two bound water layers is obtained from experimental dielectric data of hydrated lysozyme.[30] Although this response is used to model bound water, it will also contain contributions from mobile, polar side chains located on the protein surface. The dark solid line in Figure 6 is the spectral density of model II and shows the decreased magnitude of the aqueous solvation contribution to the response. The peak shift simulations with and without intramolecular contributions using the model II spectral density are shown in Figures 7 and 8, respectively. Model II clearly provides a better representation of the long time behavior. The third model treats the entire lysozyme macromolecule and the first two water layers with the same frequency-dependent dielectric response as the experimentally determined dielectric data of hydrated lysozyme.[30] Again, the dashed line in Figure 6 shows the spectral density and those in Figures 7 and 8 are the peak shifts calculated using model III. It is important to note that the relative contribution from bulk water is significantly smaller when the lysozyme dielectric response is considered in the model. The simulation based on the third model also closely resembles the experimental data. Moreover, the simulations of model II and model III are quite similar. The fourth model treats the entire lysozyme complex using the dielectric response from the molecular dynamics simulation of lysozyme,[24] assumed to be uniform throughout the protein, and the dielectric response of bulk water for all the surrounding water.[47] A single Debye relaxation dominates the model IV spectral density (see Figure 6) and fails to capture the complex nature of the long time solvation dynamics (see Figures 7 and 8).

IV. Discussion

The three-pulse photon echo peak shift technique is an incisive probe of the interactions of a chromophore with the aqueous protein environment. We extend the success of continuum models in characterizing an arbitrary charge distribution in a dielectric cavity to macromolecules such as lysozyme. The present study uses physically reasonable dielectric con-

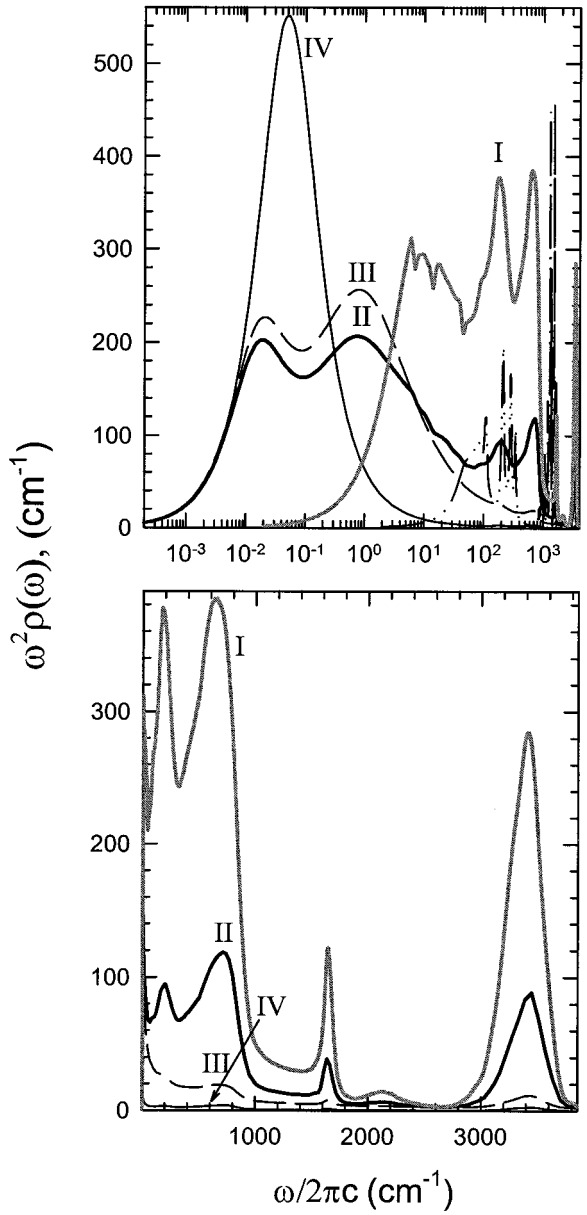

Figure 6. Spectral densities for the transition frequency correlation function of the aqueous lysozyme complex. Each model I, II, III, and IV corresponds to those in Figure 5. The dashed−dotted black lines represent the spectral densities of the intramolecular vibrations of eosin. See text for calculation details.

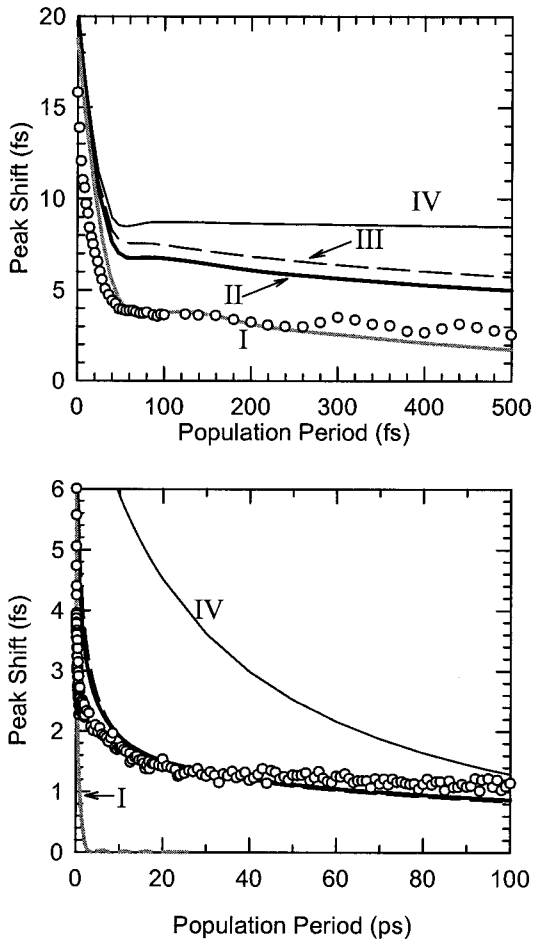

Figure 7. Aqueous lysozyme complex experimental peak shift (circles) and calculated peak shift (lines). The simulations include only intermolecular motions and thus should not be accurate at short times (upper panel). However, simulations using models II and III capture much of the long time dynamics (lower panel).

tinuum models to interpret the 3PEPS measurements of eosin bound to the hydrophobic pocket of lysozyme. With these model calculations some qualitative conclusions regarding (A) the local chromophore environment, (B) the ultrafast solvation, and (C) the long time behavior of the lysozyme complex can be drawn. Finally we discuss the dynamical origins of the electronic energy fluctuations of the chromophore in the aqueous lysozyme environment.

A. The Local Chromophore Environment. Various observations suggest that the local environment around the chromophore is different when eosin is bound to lysozyme. Implicit in all our models is that the effective polarity of the eosin environment in the lysozyme complex is significantly reduced from that of eosin in pure water. The spectral red-shift in Figure 2 is in accord with the reduced polarity at the binding site. Another plausible origin for the red-shift of protein-bound eosin relative to eosin alone in the aqueous solution is that it arises from hydrogen bonding.[58] Two hydrogen bonds can be formed between the eosin and the tyrosine residues of lysozyme in the hydrophobic pocket. Another indication of the different local eosin environment is the different coupling strengths for eosin in water and eosin bound to lysozyme in water as revealed by the calculated coupling strengths from the experimental steady-state absorption and fluorescence spectra and corroborated by the initial value of the peak shift. The larger the initial peak shift, the smaller the chromophore−bath coupling strength. Hence, the higher initial peak shift in the aqueous lysozyme complex data (16 fs compared to 12 fs for eosin in water) suggests a decreased coupling of the chromophore's electronic transitions to the nuclear motions of its environment.

B. Ultrafast Relaxation. An ultrafast inertial response is characteristic of solutes[4,14,15,59] and even electrons[3] in aqueous environments. In our previous study of aqueous solvation dynamics, there was no clear time scale separation between the intermolecular dynamics of water and those attributed to the intramolecular dynamics of the eosin probe molecule. A theoretical spectral density calculated via dielectric continuum theory allowed for identification of the individual contributions to the echo signal. We concluded that aqueous solvation dynamics exhibit a very rapid (∼30 fs) decay of the three-pulse photon echo peak shift contributing to ∼60% of the total solvent relaxation.[14] As the lower panel of Figure 3 shows, the initial dynamics in the complex appear identical to those in aqueous solvation. The question remains: to what extent do protein motions contribute to this ultrafast relaxation?

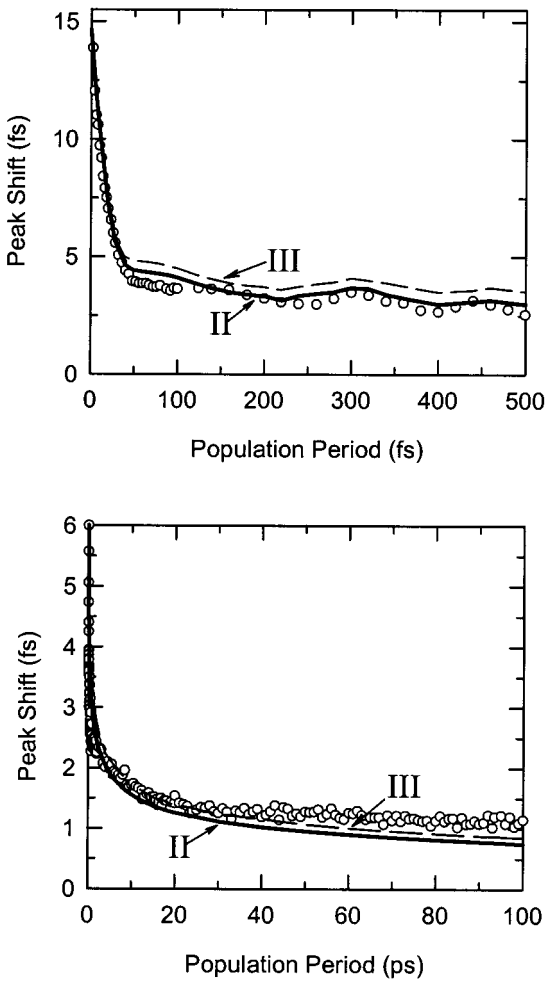

Figure 8. Aqueous lysozyme complex experimental peak shift (circles) and calculated peak shift (lines). The simulations used models II and III and include both intermolecular and intramolecular motions.

Proteins can undergo internal motions on time scales from femtoseconds to seconds.[22] Hence, it is reasonable to expect that protein modes can contribute to the overall relaxation. Several MD simulations have suggested that small amplitude, sub 100 fs relaxations occur in solvated proteins.[9,10,22,60] Low-frequency motions have also been observed in simulations of the photosynthetic reaction center.[9] In the aqueous lysozyme system, MD simulations suggest that protein atomic and velocity displacements occur on 67 and 15 fs time scales, respectively.[22,60]

To provide some experimental insight on the ultrafast time scales of lysozyme motions, an infrared spectrum was recorded down to 100 cm^{-1} on crystalline lysozyme. Features in the sub 500 cm^{-1} region were observed at 166, 242, 300, and 435 cm^{-1}. These observations are consistent with another far-infrared study on lysozyme crystals reporting a high density of modes between 240 and 450 cm^{-1} as well as two lower frequency peaks at 56 and 90 cm^{-1}.[61] Despite the presence of low-frequency lysozyme motions, the possible contribution of water associated with the lysozyme crystals makes it a challenge to separate individual contributions. The overlapping time scales of internal protein motions with both intermolecular solvent motions and intramolecular vibrational motions of the chromophore present another complication. For example, the hindered translational motion of the hydrogen-bonded network at 180 cm^{-1} overlaps the observed lysozyme peak at 166 cm^{-1} in the IR spectrum.

Despite the challenges in characterizing the ultrafast response in this protein, the peak shift data of the lysozyme complex provide substantial insight. As shown in Figure 3, a nearly identical ultrafast peak shift (<200 fs) is observed for both eosin bound to lysozyme and eosin in aqueous solution. Hence, the mechanism of the ultrafast response in the lysozyme complex is likely to be identical to that dominating aqueous solvation dynamics. Namely, the ultrafast dynamics in this aqueous protein system appears to be dominated by librational motion of bulk water molecules and not by ultrafast protein motions. This seems likely to be the case for most small soluble proteins. Experiments in methanol−water mixtures will provide an interesting test of this idea. Since methanol has a librational band at 80 cm^{-1},[52] a cleaner separation of solvent from protein motions should be possible.

C. Long Time Behavior. For many simple polar solute−solvent systems, the characteristic fluctuations corresponding to the diffusive portion of the solvation dynamics are on the order of picoseconds as revealed by both experiment[1−3,14,15,42,43,52] and theory.[5,6] However, the dynamics of the dielectric fluctuations in organized media[17−20,53−57] exhibit complex long time behavior. When the eosin/water and the eosin/lysozyme data are fit to sums of exponentials, the lysozyme complex data show additional time constants of 7 and 135 ps (or a 530 ps component for the data taken to 1 ns) not present in the aqueous environment. These values compare well to the solvation relaxation times of 4 and 270 ps obtained via dielectric spectroscopy on hydrated lysozyme. Recently, organized or restricted environments such as micelles[54,55] and reverse micelles[56,57] have been proposed as useful models for biological systems. A variety of long time components have been observed in these systems. Vajda et al. used time-resolved fluorescence to study coumarin 680 in γ-cyclodextrin in aqueous solution. They observed time constants of 13 ps, 109 ps, and 1.2 ns, which differ substantially from the response of coumarin in pure water.[54] Moreover, Levinger and co-workers resolve a long solvation time component of 100 ps in a restricted aqueous inverted micellular environment.[57] Instead of using such model systems, Boxer and co-workers probed the dynamics of a dye bound to apomyoglobin. They observed multi-exponential behavior in time-resolved fluorescence measurements but could not correlate a molecular mechanism to the observed dynamics.[53] Although theory and simulations have concluded that low-frequency motions on the picosecond time scale exist in proteins, it remains difficult to determine if these motions originate from protein motions, from motions of bound water, or from some combination of the two.

Without a model, a simple exponential fit to the solvation time correlation function or peak shift cannot provide a molecular mechanism to characterize aqueous protein solvation. In the present study, several dielectric models and their corresponding spectral densities are employed to parametrize the nonexponential relaxation of the lysozyme and used to simulate the peak shift data. Not unexpectedly, model I, whose only contribution to the frequency-dependent dielectric function is that of bulk water, fails to capture the long time dynamics of the lysozyme complex. Model II includes the dielectric response of the two layers of water associated with lysozyme and performs reasonably well in capturing the long time behavior. Model III includes the influence of the lysozyme on the dynamics in addition to the two layers of bound water, and like model II captures much of the long time dynamics of the peak shift. As shown in Figures 7 and 8, model III slightly improves the simulation of the peak shift data in the intermediate time range, suggesting that the origin of the long time component in

protein solvation involves both the lysozyme and the water associated with the protein. Although the spectral densities for models II and III have very different amplitudes in the high and low-frequency ranges, the corresponding simulated peak shifts are quite similar. More experimental and theoretical studies are required to differentiate more clearly between models II and III. Hence, with the current models, distinguishing the dielectric relaxation of protein groups from that of tightly bound water molecules on the protein surface is a challenge. The simulation of the peak shift data using the model IV spectral density indicates that current MD simulations fail to describe either the time scale or the amplitude of the dielectric relaxation of the aqueous lysozyme complex. At present, the spectral density relevant to fluctuations in the electronic energy gap of a protein-bound chromophore does not seem accessible from simulation alone.

To compare the experimental echo signal, a convolution with a finite pulse duration is required. It is the pulse width effect that prevents us from distinguishing small amplitude differences in the spectral density. In this regard, the generation of shorter visible pulses can aid in differentiating the spectral densities of models II and III. However, the electronic transition frequency correlation function, $M(t)$, is more sensitive to small amplitude changes in the spectral density since $M(t)$ is the time-dependent first moment of the spectral density

$$M(t) = \frac{1}{\pi\lambda}\int_0^\infty d\omega\omega\rho(\omega)\cos(\omega t) \qquad (3)$$

$M(t)$ was calculated using model I−IV spectral densities and is shown in Figure 9. Hence, we propose a combination of echo measurements and time-resolved fluorescence Stokes shift measurements to measure $S(t)$, equivalent to $M(t)$ in the classical limit, and provide an additional experimental observable for comparison with the various model spectral densities. The calculation of both the 3PEPS and $s(t)$ should also allow for a systematic test of the various dielectric measurements on complex macromolecular systems. Furthermore, experiments with covalently attached chromophores will allow access to a wider range of experimental conditions and lead to a productive feedback between theory and experiments.

V. Concluding Remarks

Although the contributions from internal protein motions to the dielectric response of the aqueous lysozyme complex are far from being completely characterized, a number of conclusions can be drawn. First, it seems likely that the electronic energy gaps of chromophores within small aqueous proteins will fluctuate with the same ultrafast time scale as is observed for directly solvated chromophores. For many aqueous macromolecular systems, the fast motion of the protein may contribute negligibly. On a longer time scale, the protein certainly does contribute significantly, either directly through motions of polar side chains or indirectly through the water bound to such groups at the protein surface. Current molecular dynamics simulations do not seem to capture the complexity of this slower portion of the response.

Acknowledgment. Experimental aspects of this collaborative research were supported by the National Science Foundation. Theoretical aspects carried out by X.S. were supported by the U.S. Department of Energy, Office of Basic Energy Science (grant number FDDE-FG03-87ER13793). X.J.J. thanks Dr. Michael Martin and Beamline 1.4 (Advanced Light Source, LBNL) for use of the IR spectrometer and Professor Heinz Frei for insightful suggestions regarding the IR measurement. Dr. Gerry McDermott is acknowledged for assistance with the molecular modeling program O used to generate Figure 1. X.S. is grateful to Professors David Chandler and Rudy Marcus for their discussion and encouragement.

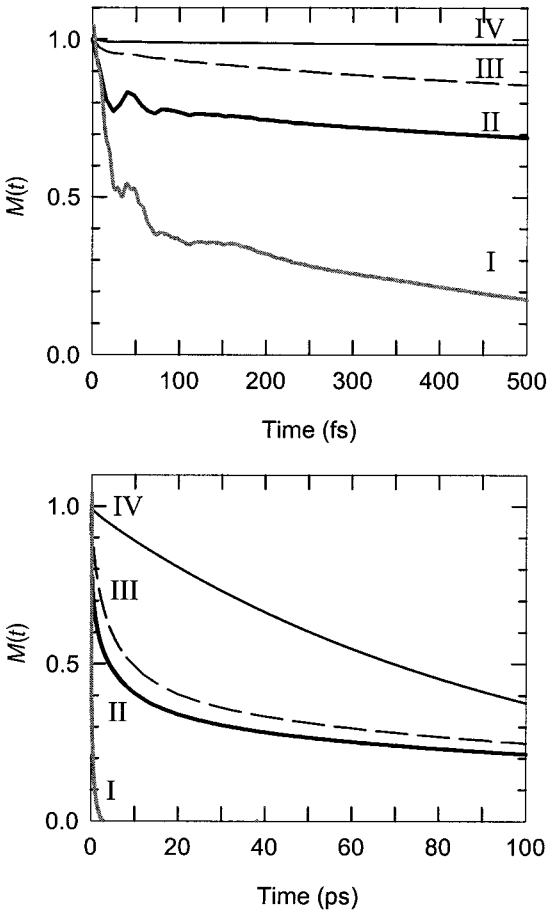

Figure 9. The transition frequency correlation function $M(t)$ calculated using eq 3 with the spectral densities whose labels correspond to those of Figure 6.

Appendix: Extraction of the Reorganization Energy from Absorption and Fluorescence Spectra

A new and useful relationship is established between the reorganization energy and absorption and fluorescence spectra. The traditional method for estimating the reorganization energy assumes these spectra have Gaussian shapes. In contrast, the relationship given here follows exactly from the condition that the dielectric medium obeys linear response.

In solvation dynamics, the reorganization energy is widely used as a measure of the strength of interactions between a chromophore and its surrounding dielectric media.[1−3] Traditionally, this quantity is estimated from the Stokes shift, which is the frequency difference between the absorption spectrum maximum and the associated fluorescence spectrum maximum. In particular, the reorganization energy (λ) is taken to be half of the Stokes shift.[49,62] Namely,

$$\lambda = \frac{1}{2}\hbar[\max\{\sigma_a(\omega)\} - \max\{\sigma_f(\omega)\}] \qquad (A1)$$

where $\sigma_a(\omega)$ and $\sigma_f(\omega)$ are the experimentally measured absorption and fluorescence spectra, normalized according to the spectrum maximum, and $\max\{\cdots\}$ denotes the frequency at the spectra maximum. But this estimate is accurate only if the

absorption and fluorescence spectra have Gaussian shapes. We present here a more accurate and easily applied relationship to estimate the reorganization energy from the absorption and fluorescence spectra. The only assumption used in this method is that polarization fluctuations of the dielectric medium follow Gaussian statistics.

We suppose the chromophore has two electronic states, the ground state $|g\rangle$ and the excited state $|e\rangle$. Since the dielectric medium surrounding the chromophore obeys linear response, the dielectric response of this medium can be described phenomenologically as a harmonic bath. The Hamiltonian of the system assumes the following form[49]

$$H = |g\rangle H_g \langle g| + |e\rangle H_e \langle e| \tag{A2a}$$

with

$$H_g = \frac{1}{2}\sum_i \hbar\omega_i [p_i^2 + q_i^2] \tag{A2b}$$

and

$$H_e = \hbar\omega_{eg}^0 + \frac{1}{2}\sum_i \hbar\omega_i [p_i^2 + (q_i + d_i)^2] \tag{A2c}$$

where H_g is the effective harmonic bath with dimensionless momentum p_i and coordinate g_i for a mode at frequency ω_i. H_e is the harmonic bath shifted by d_i for mode i due to interaction with the chromophore, and $\omega_{eg}{}^0$ is the transition frequency of the chromophore in vacuum. As usual, the spectral density is defined as

$$\rho(\omega) \equiv \frac{1}{2}\sum_i d_i^2\, \delta(\omega - \omega_i) \tag{A3}$$

With the above definition, the absorption and fluorescence line shapes are given by[49]

$$\sigma_a(\tilde{\omega} + \omega_{eg}) = \frac{1}{\pi}\,\mathrm{Re}\int_0^\infty dt\, \exp[i\tilde{\omega}t - g(t)] \tag{A4}$$

$$\sigma_f(\tilde{\omega} + \omega_{eg}) = \frac{1}{\pi}\,\mathrm{Re}\int_0^\infty dt\, \exp[i\tilde{\omega}t - g^*(t)] \tag{A5}$$

where $\tilde{\omega} = \omega - \omega_{eg}$. Here, ω_{eg} is the frequency where the absorption and fluorescence spectra intersect as indicated in the upper panel of Figure 2, $g(t)$ is the usual line broadening function,

$$g(t) = g'(t) + ig''(t) \tag{A6a}$$

$$g'(t) = \int_0^\infty d\omega(1 - \cos\omega t)\coth(\beta\hbar\omega/2)\rho(\omega) \tag{A6b}$$

$$g''(t) = \int_0^\infty d\omega\, \sin(\omega t)\, \rho(\omega) \tag{A6c}$$

and $g^*(t)$ is complex conjugate of $g(t)$. Furthermore, the reorganization energy is

$$\lambda = \hbar\omega_{eg} - \hbar\omega^0{}_{eg} = \hbar\int_0^\infty d\omega\omega\rho(\omega) \tag{A7}$$

If the frequency axis is shifted by ω_{eg}, eqs A4 and A5 can be written as

$$\sigma_a(\tilde{\omega}) + \sigma_f(\tilde{\omega}) = \frac{1}{\pi}\int_0^\infty dt\, \exp[-g'(t)]\cos g''(t)\cos\tilde{\omega}t \tag{A8}$$

$$\sigma a(\tilde{\omega}) - \sigma f(\tilde{\omega}) = \frac{1}{\pi}\int_0^\infty dt\, \exp[-g'(t)]\sin g''(t)\sin\tilde{\omega}t \tag{A9}$$

The inverse Fourier transforms of eqs A8 and A9 yield

$$R(t) \equiv \exp[-g'(t)]\cos g''(t) = 2\int_0^\infty d\tilde{\omega}\cos\tilde{\omega}t\,[\sigma_a(\tilde{\omega}) + \sigma_f(\tilde{\omega})] \tag{A10}$$

$$I(t) \equiv \exp[-g'(t)]\sin g''(t) = 2\int_0^\infty d\tilde{\omega}\sin\tilde{\omega}t[\sigma_a(\tilde{\omega}) - \sigma_f(\tilde{\omega})] \tag{A11}$$

From the definition of λ given in eq A7 and the definition of $g''(t)$ given in eq A6c, we find

$$\begin{aligned}\lambda t &= \hbar\lim_{t\to 0} g''(t)\\ &= \hbar\lim_{t\to 0}\tan^{-1}\frac{I(t)}{R(t)}\\ &= \hbar\frac{\int_0^\infty d\tilde{\omega}[\sigma_a(\tilde{\omega}) - \sigma_f(\tilde{\omega})]\tilde{\omega}}{\int_0^\infty d\tilde{\omega}[\sigma_a(\tilde{\omega}) + \sigma_f(\tilde{\omega})]}t\end{aligned} \tag{A12}$$

Thus,

$$\lambda = \hbar\frac{\int_0^\infty d\tilde{\omega}[\sigma_a(\tilde{\omega}) - \sigma_f(\tilde{\omega})]\tilde{\omega}}{\int_0^\infty d\tilde{\omega}[\sigma_a(\tilde{\omega}) + \sigma_f(\tilde{\omega})]} \tag{A13}$$

If the absorption and fluorescence spectra are Gaussian in shape, the traditional estimate of the reorganization energy is recovered from eq A12. However, for non Gaussian spectra, eq A12 gives a result for λ that differs from the traditional estimate. The absorption and fluorescence spectra for the lysozyme complex in water are shown in the upper panel of Figure 2. Their shapes differ significantly from Gaussian. According to the traditional estimate, the reorganization energy is half of the Stokes shift, or 330 cm^{-1}. In contrast, the implementation of eq A12 gives 710 cm^{-1}. Thus, for this representative system, the traditional estimate deviates by more than a factor of 2. The eosin in water system is another example: our estimate of the reorganization energy gives 877 cm^{-1} versus 359 cm^{-1} calculated using the traditional method.[14] Hence, this new method should give a better estimate of the reorganization energy.

It should be noted that $\sigma_a(\tilde{\omega}) - \sigma_f(\tilde{\omega})$ and $\sigma_a(\tilde{\omega}) + \sigma_f(\tilde{\omega})$ will be odd and even functions of $\tilde{\omega}$, respectively (cf. eqs A8 and A9). To the extent that the dielectric medium responds linearly, deviations of $\sigma_a(\tilde{\omega}) - \sigma_f(\tilde{\omega})$ and $\sigma_a(\tilde{\omega}) + \sigma_f(\tilde{\omega})$ from being odd and even functions, respectively, indicate nonlinear behavior of the bath. This behavior includes the intramolecular vibrations of the chromophore, since the experimentally measured absorption and fluorescence spectra cannot differentiate the broadening due to intramolecular or solvent contributions. However, the reorganization energy obtained from our method contains both contributions. In a particular situation when the separation between the intramolecular and solvent contribution is involved, Mertz has expressed the reorganization energy in terms of the first moment of the absorption and fluorescence

spectra.[63,64] However, our formulation is significantly different since the only assumption made is that the medium obeys linear response.

References and Notes

(1) Fleming, G. R.; Cho, M. *Annu. Rev. Phys. Chem.* **1996**, *47*, 109 is a comprehensive review of solvation dynamics.

(2) For a reivew of optical Kerr, dielectric, and Stoke shift measurements used to probe solvation dynamics refer to: Castner, E. W., Jr.; Maroncelli, M. *J. Mol. Liq.* **1998**, *77*, 1.

(3) For a recent review of solvation dynamics studied using photon echo spectroscopy refer to: de Boeij, W. P.; Pshenichnikov, M. S.; Wiersma, D. A. *Annu. Rev. Phys. Chem.* **1998**, *49*, 99.

(4) Roy, S.; Bagchi, B. *J. Chem. Phys.* **1993**, *99*, 9938.

(5) Raineri, F. O.; Resat, H.; Baw-Ching, P.; Hirata, F.; Friedman, H. L. *J. Chem. Phys.* **1994**, *100*, 1477.

(6) Song, X. Y.; Chandler, D.; Marcus, R. A. *J. Phys. Chem.* **1996**, *100*, 11954.

(7) Song, X. Y.; Chandler, D. *J. Chem. Phys.* **1998**, *108*, 2594.

(8) Stratt, R. M.; Maroncelli, M. *J. Phys. Chem.* **1996**, *100*, 12981.

(9) Gehlen, J. N.; Marchi, M.; Chandler, D. *Science* **1994**, *263*, 499.

(10) Schulten, K.; Tesch, M. *Chem. Phys.* **1991**, *158*, 421.

(11) Kohen, A.; Klinman, J. P. *Acc. Chem. Res.* **1998**, *31*, 397.

(12) Rector, K. D.; Rella, C. W.; Hill, J. R.; Kwok, A. S.; Sligar, S. G.; Chien, E. Y. T.; Dlott, D. D.; Fayer, M. D. *J. Phys. Chem. B.* **1997**, *101*, 1468.

(13) Lim, M.; Jackson, T. A.; Anfinrud, P. A. *Proc. Natl. Acad. Sci., U.S.A.* **1993**, *90*, 8302.

(14) Lang, M. J.; Jordanides, X. J.; Song, X.; Fleming, G. R. *J. Chem. Phys.* **1999**, *110*, 5584.

(15) Jimenez, R.; Fleming, G. R.; Kumar, P. V.; Maroncelli, M. *Nature* **1994**, *369*, 471.

(16) Nandi, N.; Bagchi, B. *J. Phys. Chem. B* **1997**, *101*, 10954.

(17) Joo, T. H.; Jia, Y. W.; Yu, J. Y.; Jonas, D. M.; Fleming, G. R. *J. Phys. Chem.* **1996**, *100*, 2399.

(18) Jimenez, R.; Dikshit, S. N.; Bradforth, S. E.; Fleming, G. R. *J. Phys. Chem.* **1996**, *100*, 6825.

(19) Groot, M. L.; Yu, J. Y.; Agarwal, R.; Norris, J. R.; Fleming, G. R. *J. Phys. Chem. B* **1998**, *102*, 5923.

(20) Homoelle, B. J.; Edington, M. D.; Diffey, W. M.; Beck, W. F. *J. Phys. Chem. B* **1998**, *102*, 3044.

(21) Fraga, E.; Loppnow, G. R. *J. Phys. Chem. B* **1998**, *102*, 7659.

(22) Brooks, C. L.; Karplus, M.; Pettitt, B. M. *Proteins: A Theoretical Perspective of Dynamics, Structure, and Thermodynamics*; J. Wiley: New York, 1988.

(23) King, G.; Lee, F. S.; Warshel, A. *J. Chem. Phys.* **1991**, *95*, 4366.

(24) Smith, P. E.; Brunne, R. M.; Mark, A. E.; Van Gunsteren, W. F. *J. Phys. Chem.* **1993**, *97*, 2009.

(25) Simonson, T.; Brooks, C. L. *J. Am. Chem. Soc.* **1996**, *118*, 8452.

(26) Laogun, A. A. *J. Mol. Liq.* **1986**, *32*, 111.

(27) Miura, N.; Asaka, N.; Shinyashiki, N.; Mashimo, S. *Biopolymers* **1994**, *34*, 357.

(28) Amo, Y.; Karube, I. *Biosens. Bioelectron.* **1997**, *12*, 953.

(29) Bonincontro, A.; Francesco, A. D.; Onori, G. *Chem. Phys. Lett.* **1999**, *301*, 189.

(30) Harvey, S. C.; Hoekstra, P. *J. Phys. Chem.* **1972**, *76*, 2987.

(31) Bone, S.; Pethig, R. *J. Mol. Biol.* **1982**, *157*, 571.

(32) Careri, G. G. M.; Giansanti, A.; Rupley, J. A. *Proc. Natl. Acad. Sci., U.S.A.* **1985**, *82*, 5342.

(33) Fullerton, G. D.; Ord, V. A.; Cameron, I. L. *Biochim. Biophys. Acta* **1986**, *869*, 230.

(34) Lioutas, T. S.; Baianu, I. C.; Steinberg, M. P. *Arch. Biochem. Biophys.* **1986**, *247*, 68.

(35) Pethig, R. *Annu. Rev. Phys. Chem.* **1992**, *43*, 177.

(36) Svergun, D. I.; Richard, S.; Koch, M. H. J.; Sayers, Z.; Kuprin, S.; Zaccai, G. *Proc. Natl. Acad. Sci., U.S.A.* **1998**, *95*, 2267.

(37) Grant, E. H.; Sheppard, R. J.; South, G. P. *Dielectric Behavior of Biological Molecules*; Oxford: Clarendon, 1978.

(38) Kepka, A. G.; Grossweiner, L. I. *Photochem. Photobiol*. **1973**, *18*, 49.

(39) Baugher, J. F.; Grossweiner, L. I.; Lewis, C. J. *J. Chem. Soc., Faraday Trans 2* **1974**, *70*, 1389.

(40) Chang, M. C.; Cross, A. J.; Fleming, G. R. *J. Biomol. Struct. Dyn*. **1983**, *1*, 299.

(41) Cross, A. J.; Fleming, G. R. *Biophys. J*. **1983**, *50*, 507.

(42) Joo, T.; Jia, Y.; Yu, J.-Y.; Lang, M. J.; Fleming, G. R. *J. Chem. Phys.* **1996**, *104*, 6089.

(43) de Boeij, W. P.; Pshenichnikov, M. S.; Wiersma, D. A. *J. Phys. Chem.* **1996**, *100*, 11806.

(44) Blake, C. F.; Koenig, D. F.; Mair, A. C.; North, A. T.; Phillips, D. C.; Sarma, V. R. *Nature* **1965**, *206*, 757.

(45) Reed, M. K.; Armas, M. S.; Steinershepard, M. K.; Negus, D. K. *Opt. Lett.* **1995**, *20*, 605.

(46) Ramanadham, M.; Sieker, L. C.; Jensen, L. H. *Acta Crystallogr. Sect. B* **1990**, *46*, 63.

(47) See Figure 1 of Song, X. Y.; Marcus, R. A. *J. Chem. Phys.* **1993**, *99*, 7768 for a complete set of dielectric data of water.

(48) Lee, B.; Richards, R. M. *J. Mol. Biol.* **1971**, *55*, 379.

(49) Mukamel, S. *Principles of Nonlinear Optical Spectroscopy*; Oxford University Press: New York, 1995.

(50) Cho, M.; Yu, J.-Y.; Nagasawa, Y.; Passino, S. A.; Fleming, G. R. *J. Phys. Chem.* **1996**, *100*, 11944.

(51) Book, L. D.; Scherer, N. F. *J. Chem. Phys.* **1999**, *111*, 792.

(52) Passino, S. A.; Nagasawa, Y.; Joo, T.; Fleming, G. R. *J. Phys. Chem.* **1996**, *101*, 725.

(53) Pierce, D. W.; Boxer, S. G. *J. Phys. Chem.* **1992**, *96*, 5560.

(54) Vajda, S.; Jimenez, R.; Rosenthal, S. J.; Fidler, V.; Fleming, G. R.; Castner, E. W. *J. Chem. Soc. Faraday Trans.* **1995**, *91*, 867.

(55) Sarkar, N.; Datta, A.; Das, S.; Bhattacharyya, K. *J. Phys. Chem.* **1996**, *100*, 15483.

(56) Mittleman, D. M.; Nuss, M. C.; Colvin, V. L. *Chem. Phys. Lett.* **1997**, *275*, 332.

(57) Riter, R. E.; Willard, D. M.; Levinger, N. E. *J. Phys. Chem. B* **1998**, *102*, 2705.

(58) Fowler, G. J. S.; Visschers, R. W.; Grief, G. G.; van Grondelle, R.; Hunter, C. N. *Nature* **1992**, *355*, 848.

(59) Maroncelli, M.; Fleming, G. R. *J. Chem. Phys.* **1988**, *89*, 5044.

(60) Brooks, C. L.; Karplus, M. *J. Mol. Biol.* **1989**, *208*, 159.

(61) Ataka, M.; Tanaka, S. *Biopolymers* **1979**, *18*, 507.

(62) Reynolds, L.; Gardecki, J. A.; Frankland, S. J. V.; Horng, M. L.; Maroncelli, M. *J. Phys. Chem.* **1996**, *100*, 10337.

(63) Mertz, E. L. *Chem. Phys. Lett.* **1996**, *262*, 27.

(64) Mertz, E. L.; German, E. D.; Kuznetsov, A. M. *Chem. Phys.* **1997**, *215*, 355.